RESEARCH ON FRACTURE OF FIBRE REINFORCED CONCRETE SUBJECTED TO COMBINED STRESS

Professor **Antanas Žiliukas, Ph.D**
Department of Mechanics and Solids,
Kaunas University of Technology,
Kestučio st. 27, LT- 44025, Kaunas, Lithuania
E-mail: antanas.ziliukas@ktu.lt

Lecturer **Algirdas Augonis, Ph.D**
Department of Building Materials,
Kaunas University of Technology,
Studentu st. 48, LT-51367, Kaunas, Lithuania
E-mail: algirdas.augonis@ktu.lt

Abstract. Major methodologies that are used to determine fracture properties of concrete have been developed for the cases of simple loads, for instance a three-point bending test. However, these test methods are not always suitable in the cases of combined stresses and strains or combined loads. Therefore, a method of calculating the characteristic length of concrete with fictitious crack according to characteristic volume is proposed in this article. To this end cross-shaped concrete specimens with fictitious crack were used. The concrete was reinforced with steel or polypropylene fibres. Ultimate load, vertical strain (deflection) and Crack Mouth Opening Displacement (CTOD) were measured in experimental tests.

Keywords: characteristic length, characteristic volume, fracture energy, CMOD, fibres.

1. Introduction

Linear fracture mechanics is a recent branch of science that started developing in the beginning of the 20th century. At first it was applied to ultra brittle materials. Later it was successfully applied in metal fracture prediction and evaluation. Meanwhile, the first concrete fracture tests were conducted in 1960s. Fracture tests were usually conducted with concrete specimens of standard dimensions with a fictitious crack (Fictitious Crack Model). Because of low tensile strength of concrete the most popular were crack mouth displacement tests where stress intensity factor K_I is calculated according to critical load. Factor K_I is calculated from analytical equations; however, it is suitable only for specimens with limited area boundary conditions and dimensions (Ioannides, 2006; Yon et al., 1997).

Critical strain energy release rate (G_C) and K_C criteria are exclusively applied for linear elastic fracture behaviour (Bakar and Skrzypek 2007). Critical strain energy release rate or effective fracture energy G_C required for crack propagation is a criterion of key importance in concrete fracture mechanics. Theoretically, this energy is proportional to the square of stress intensity factor; however, effective fracture energy levels observed in experimental tests with concrete were significantly higher. This can be explained by the fact that concrete is heterogeneous material with numerous micro defects which at certain space above the crack tip absorb most of the energy. This space was called FPZ (Fracture Process Zone). A conclusion was made that in ultra brittle materials (glass, ceramics) FPZ length from the tip of the crack is very short and increases with fracture plasticity (Hu and Duan 2004).

Interestingly, the very existence of cohesive stresses over the main crack surface in concrete requires a nonzero FPZ height. This is because the cohesive or crack bridging stresses in concrete have to come from a frictional pull out of aggregates and a tearing of various unbroken connections over the uneven main crack surface created by multiple cracking, which occurs in FPZ of certain length and height (Hu and Duan 2004).

It is hard to determine this zone in experimental tests, however according to the recently published research data FPZ length in ordinary concrete is 90 mm and the width is ~ 35 mm. Theoretically FPZ length can be calculated by means of another concrete fracture criterion called characteristic length l_{ch}. However, theoretically calculated characteristic length is 2 – 3 times longer than the actual FPZ length (Hadjab-Souag et al. 2007).

Actually, there are more criteria used to estimate concrete fracture available in published articles in order to obtain the most accurate estimation of concrete fracture with respect to its structure and nonlinear properties. Nevertheless, the classical criteria, irrespective of their drawbacks, have remained the most popular among the researchers of concrete fracture mechanics because of accumulated information, clear methodology and other possible reasons (Zhang and Wu, 1999). Although concrete fracture mechanics test methods are established for standard concrete specimens, fracture criteria for concrete specimens of more complex forms are hard to establish; after all, in reality concrete fracture is a 3D process. With the development of computing techniques more sophisticated tests will undoubtedly be conducted in order to make concrete fracture more predictable and estimable.

Cracking in concrete initiates and propagates in the direction of the major principal strain starting from the section, where the first crack originates (Khalfallah, 2008).

The main purpose of this paper is to identify the fracture patterns in concrete specimens with initial fictitious cracks and to create a methodology for fracture characterization in concretes subjected to combined stress. Another aim is to identify the change in fracture characteristics of concrete reinforced with different types of fibres.

To obtain a three-dimensional state of combined stress a seamless cross-shaped specimen with a crack was selected and subjected to a vertical external load. A numerical model of this specimen was developed in order to identify the distribution of adverse stresses in the specimen.

Mechanical properties and fracture parameters of concrete specimens with fictitious cracks under load were determined experimentally by means of Toni-Technik computer controlled hydraulic press and deflection transducers, whereas fracture criteria were calculated according to the theory of linear fracture mechanics.

In the process of fracture in fibre reinforced composite (FRC) materials, fibres bridging the cracks in the matrix can provide resistance to crack propagation and opening until they are pulled out or stressed to rupture. Consequently, FRC materials may be insensitive to the presence of notches, depending on the effectiveness of the reinforcement. The material zone which undergoes inelastic deformation associated with fibre bridging is often called the process zone. The process zone of FRC can be extremely large, and its size depends on the structural geometry and loading condition. A lot of energy is absorbed in the process zone during FRC fracture process (Wang, 1998).

The main factors influencing the tensile strength of steel fibre reinforced materials (SFRC) are as follows: volume and distribution of steel fibres in principal section, anchorage of fibre in concrete matrix, yield strength of fibre and strength of concrete (Salna and Marciukaitis, 2007). Concrete specimens reinforced with different polypropylene and steel fibres were used to determine the effect of fibres.

2. Concrete mixes and test methods

Dry aggregates were used to produce cement mixes for the tests. Cement and dry aggregates were dosed by weight, water and chemical agents were dosed by volume. Chemical agents were mixed in with water used to prepare the paste. Chemical agents were added to concrete mix at 1,0 wt%.

Six concrete mixes differing by type and amount of fibres (see Table 2) were used. A fibreless mix was also used as to estimate the effect of fibres on specimen. All concrete mixes were made of Portland cement CEM I 42.5 R, gravel of 4/16 fraction, sand of 0/4 fraction and water. Reba mix F2 superplasticizer was also used. Concrete mixes used in the test are presented in Table 1.

Table 1 Concrete mixes with and without fibres

Marking	Concrete mix, kg/m^3					
	Fibres	Cement	Gravel 4/16	Sand 0/4	Water	Reba mix F2
Mix 1	-	355	930	950	172	3,55
Mix 2	4	354	928	948	172	3,54
Mix 3	8	354	927	947	171	3,54
Mix 4	11	353	926	946	171	3,53
Mix 5	20	352	922	942	171	3,52
Mix 6	20	352	922	942	171	3,52
Mix 7	20	352	922	942	171	3,52

Table2 Description and conventional marking of fibres

Marking of fibres	Amount of fibres in the mix, kg/m^3	Fibre characteristics	
		Mechanical properties of the material	Form, diameter and length
Mix 2	4	Transparent extruded polypropylene, elasticity limit of 250 N/mm^2	Length 1=40 mm, width a=~ 1,1 mm, height d=0, 7~0, 8 mm. Number of waves in each fibre - 9… 10.
Mix 3	8		
Mix 4	11	Tempered steel fibres with bent ends and short polypropylene fibres	l=40 mm, d=0, 75~0, 8 mm (1/d~80). The length of short polypropylene fibres 12 mm.
Mix 5	20	Same as above without short polypropylene fibres	Same as above without short polypropylene fibres.
Mix 6	20	Low carbon steel fibres with bent ends. Tensile strength 1000 N/mm^2	1=50 mm, d=1,0 mm (1/d=50)
Mix 7	20	Rolled steel St 52-3 (DIN 17100), tensile strength 800…980 N/mm^2	Steel filling angled 20º with sharp edges. 1=32 mm, a= ~ 3,8 mm, height d=0,1~0,15 mm. Deviation of measurements is low.

To improve fracture toughness of concrete various types of fibres were used in the tests described in this article. Fibre description and conventional marking is presented in Table 2. Visual illustration of fibres is presented in photos (Figure 1).

100×100×300 mm beams were made in order to determine elasticity modulus and tensile strength of concrete using a three-point bending test. Cross-formed specimens were cast in a specially designed metal form to obtain the conditions of combined stress (Figure 2). Internal dimensions of the form: 300 mm length in both perpendicular directions, two steps of 100 mm each make the total height of 200 mm. All concrete specimens cast in these moulds were compacted by vibration.

Fig.1 Top – Dra (left) and Har (right) fibres; Bottom – 50×1.00 (left) and Poliprop (right) fibres

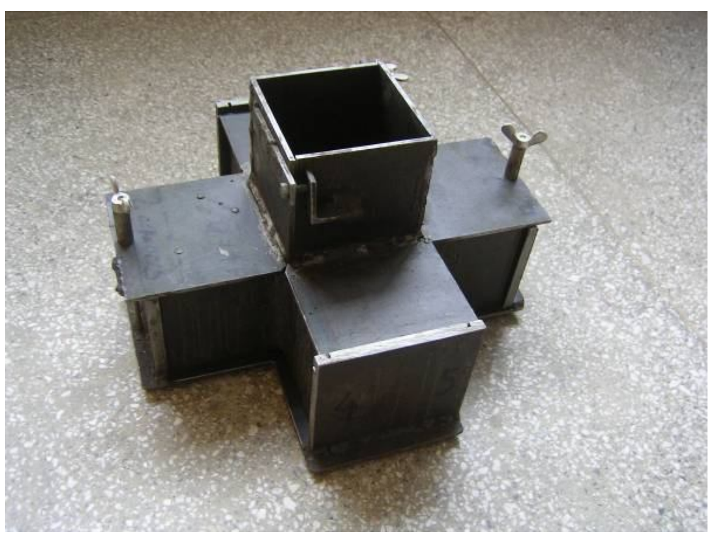

Fig.2 Metal form

To obtain 30 mm deep and 140 mm long fictitious cracks in cross-formed specimens, rectangular plastic plates of appropriate dimensions were glued on the bottom of the steel mould and were removed after the specimens settled.

After setting all specimens were kept in covered forms for 24 hours. Afterwards the specimens were removed from the moulds and cured in water (at 20 ± 2 ºC) for 27 days.

Cross-shaped specimens were subjected to compressive load applied on the top surface. Because the specimen consisted of two perpendicular prisms it was supported by four steel cylinders at the edges. The distance between the supports was the same (midspan 270 mm) in both perpendicular directions.

To maintain a steady speed of vertical strain the load was controlled automatically (it was increased or decreased). The vertical strain speed of loaded specimens was 0.4 mm/min.

In addition to vertical strain, crack mouth opening displacement was also measured by means of horizontal displacement transducer.

3. Test results

Concrete specimens of the same shape with fictitious crack surface oriented at 45 degrees were tested. All specimens made of different concrete mixes had 2 mm wide and 140 mm long fictitious cracks going along the entire specimen seen in Figure 3. Figure 3 also shows the numerical model with distribution of concrete tensile stress. The numerical model revealed that tensile stress occurs not only around crack tip but also around specimen edges located perpendicularly to the crack.

Concrete has micro cracks and voids. In concrete fracture not only values of tensile stress are important but the stress distribution as well (Žiliukas and Augonis, 2007).

As mentioned above, all concrete specimens were identical by form, only the content of the concrete was different. Tests were conducted with the aim to find out the effect of different fibre types on the fracture of concrete specimen with fictitious crack subjected to combined stress.

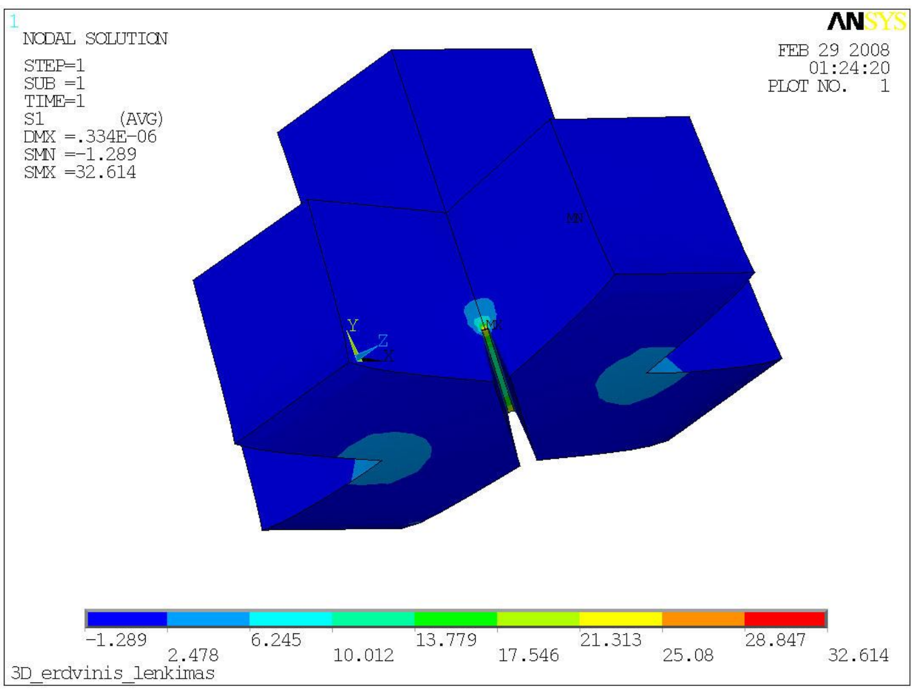

Fig.3 Distribution of tensile stress tension in the analyzed model of concrete

Fibreless specimens with a 45-degree inclined crack subjected to combined stress collapsed at the first peak stress because the crack caused by the stress at one of the two edges of the specimen connected with the propagating initial fictitious crack. In fibre reinforced concrete specimens some fibres were able to stop the propagation of the fictitious crack until the second peak stress when corners of the specimen cracked perpendicular to the fictitious crack (see Figure 4). The values measured during the test (ultimate load, vertical strain, crack initiation time and bottom crack width $CMOD_C$) are presented in Tables 3 and 4.

Fibreless (Mix 1)

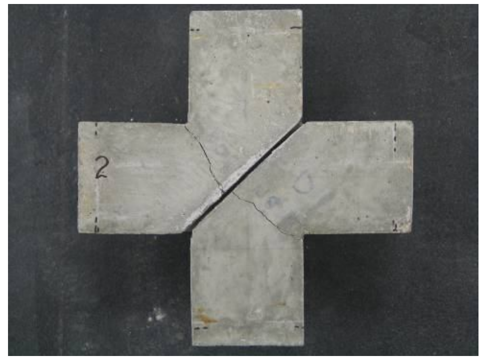

Poliprop 1 (Mix 2)

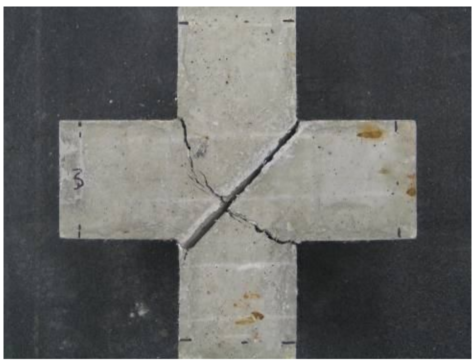

Dra 1 (Mix 4)

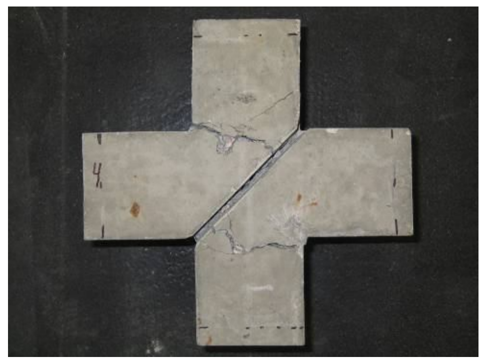

50×1.00 (Mix 6)

Fig. 4 Different fracture patterns in tested specimens due to the effect of different fibre types or amounts

Table 3 Mechanical features and fracture parameters at the first peak

Marking	Fracture energy of the cross, kN	Vertical strain, µm	CMOD, µm	Crack initiation time, s
Mix 1	22,9	115	75	38
Mix 2	24,4	126	59	38
Mix 3	19,8	221	173	63
Mix 4	23,3	194	281	58
Mix 5	34,0	218	151	57
Mix 6	28,8	118	143	39
Mix 7	24,3	161	138	44

The use of polypropylene fibres in concrete had an insignificant effect on the ultimate load when the initial crack of 140 mm opened. The ultimate load increased 6% in specimens Mix 2 and 13.5% in specimens Mix 3 compared to fibreless specimens. These results might be within acceptable tolerance limits and it would be inaccurate to state that fibres have a significant effect on fictitious crack propagation because concrete has inherent flaws and the specimens were subjected to combined stress.

However, these fibres do have a significant effect on the failure process following the initiation of the first crack. Polypropylene fibres restrain further cracking and stress increases to cause specimen deformation at the same speed of 0.4 mm/min. With this stress another crack develops perpendicular to the initial fictitious crack and the second peak stress is recorded. The fracture energy is similar to the energy that initiated the first crack. For instance, in specimen

Mix 2 the fracture energy at the second peak stress was 20% lower than at the first peak, whereas in specimen Mix 3 the fracture energy at the second peak stress was 8% higher than at the first peak stress. In the case of fibreless concrete, it is impossible to compare fracture energies at the first and second peak stresses because the specimen collapsed with the opening of the first crack. Interestingly, due to big amount of fibres specimens Mix 3 experienced the third peak stress, at which the fracture energy was 12% bigger than at the first peak stress and 4% bigger than at the second peak stress. It can be explained by the big amount of fibres that restrained not only the first crack but also the second opened crack formed in perpendicular direction. Therefore, the load had to increase in order to overcome the resistance of fibres and this caused the third peak of fracture energy (Figure 5).

The use of some types of steel fibres had an apparent effect on concrete fracture energy at the opening of the initial crack. In specimens reinforced with 20 kg/m^3 of fibres (Mix 5 and Mix 6) the fracture energy at the first peak stress increased 33% and 20% respectively in comparison to fibreless concrete specimens. Therefore, we can state that these fibres function effectively in concrete subjected to combined stress even before the opening of the crack. In specimen Mix 6 fracture energy at the second peak stress was 13% bigger than at the first peak stress and in specimen Mix 5 the fracture energy was 3% lower than at the first peak stress. According to the fracture pattern of concrete reinforced with polypropylene fibres (8 kg/m^3), we can assume that bigger amount of these fibres would lead to the third peak stress.

In specimens Mix 4 reinforced with mixed type fibres the fracture energy at the first peak was the same as in fibreless concrete specimens and at the second peak the fracture energy decreased 5% in comparison with the first peak.

Although in specimens Mix 7 the fracture energy at the first peak was 6% bigger than in fibreless concrete specimens, the second crack did not open and the specimen collapsed immediately in the same way as in the case of fibreless concrete specimens. This can be explained by the fact that sharp edged fibres could not restrain crack propagation and the specimen collapsed completely.

Vertical strain increased in all concrete specimens reinforced with different types of fibres and the bottom crack width $CMOD_C$ increased in almost all specimens prior to crack formation. Vertical strains in specimens Mix 2 and Mix 3 were respectively 9% and 48% bigger compared to fibreless concrete specimens. In specimens reinforced with 4 kg/m^3 of propylene fibres the first crack initiation time did not change, whereas $CMOD_C$ decreased 21%. In specimens with double amount of propylene fibres (8 kg/m^3), $CMOD_C$ increased 57% and crack initiation time increased 40%. Fibre deformation, $CMOD_C$ and crack initiation time in these specimens were the highest at the second peak compared to the same parameters measured in specimens with other fibre types and amounts. Another interesting fact is that concrete specimens containing 8 kg/m^3 of propylene fibres retained the maximum load (22.5 kN) at vertical strain and CMOD values above 1 mm (third stress peak) while all characteristic cracks have already been formed.

Table 4 Mechanical features and parameters of fracture at the second peak

Marking	Fracture energy of the cross, kN	Vertical strain, µm	CMOD, µm	Crack initiation time, s
Mix 1	-	-	-	-
Mix 2	19,6	396	440	86
Mix 3	21,6 (22,5)*	430 (1036)*	618 (1372)*	101 (213)*
Mix 4	22,1	294	437	76
Mix 5	32,9	361	401	83
Mix 6	33,2	218	412	57
Mix 7	-	-	-	-

* The specimen Mix 3 experienced the third peak

Vertical strain prior to the first peak in specimens Mix 5, Mix 6 and Mix 7 was respectively 47%, 3% and 29% higher compared to fibreless concrete specimen, CMOD was 50%, 48% and 46% bigger and crack initiation time was 19%, 3%, and 16% longer. Vertical strain prior to the first peak in specimen Mix 5 was 40% bigger than in specimen Mix 6 while CMOD was similar in both specimens. Specimens Mix 4 reinforced with mixed type fibres were exceptional because they had the widest critical crack width that was almost 4 times (73%) wider than in fibreless specimens. Vertical strain and crack initiation time increased 41% and 34% respectively.

4. Characteristic length, volume and FPZ

Usually fracture energy G_F is calculated from the complete stress-deformation curve. Fracture energy is the amount of energy required to completely break the beam into two separate parts. Work-of-fracture A is obtained by calculating the area under the stress-deformation curve. The total fracture energy G_F (N/m) is obtained by dividing the work-of-fracture by the known cross-section area of the beam that is separated by the propagating crack (equation 1) (Bažant et al., 1996; Appa Rao and Raghu Prasad, 2004).

$$G_F = \frac{A}{b(D - a_0)} \tag{1}$$

where D is depth of the specimen; a_0 – length of the notch; b – specimen thickness.

Fracture energy can be calculated in this way only if the new surface area after cracking is known. Such calculations are simple in the case of ordinary beams (e.g. three-point bending test). For specimens subjected to combined stress such calculations become complicated because of the complex trajectory of the crack and unknown cracked section area. The same problem was faced in experimental tests described in this article.

Therefore, characteristic length can be used in order to determine concrete brittleness (Gettu et al., 1998; Zhang and Li, 2004):

$$l_{ch} = \frac{EG_F}{f_t^2} \text{ [m]} \tag{2}$$

The lower the value of l_{ch}, the higher is the brittleness of concrete. As the work-of-fracture A, which is proportional to fracture energy G_F, was the highest in fibre reinforced concrete specimens (Table 5), the equation (2) evidently shows that the same specimens will have the biggest characteristic length. From that equation the approximate tensile strength of concrete can be obtained knowing the compressive strength of concrete. Such approximation can be found in literature (Karihaloo, 1995; Guinea et al., 2002).

Table 5 Mechanical properties of concrete and work-of-fracture required to crash the specimens

Marking	Tensile strength f_t (MPa)	Modules of elasticity, E (GPa)	Work A at first peak, Nm	Total work A, Nm
Mix 1	3,45	31,532	1,622	9,7
Mix 2	3,51	29,928	1,811	10,3
Mix 3	3,52	30,804	3,017	117,5
Mix 4	3,90	31,213	3,112	31,8
Mix 5	4,21	30,613	4,775	106,0
Mix 6	3,48	30,707	2,240	42,1
Mix 7	3,80	30,885	2,345	11,7

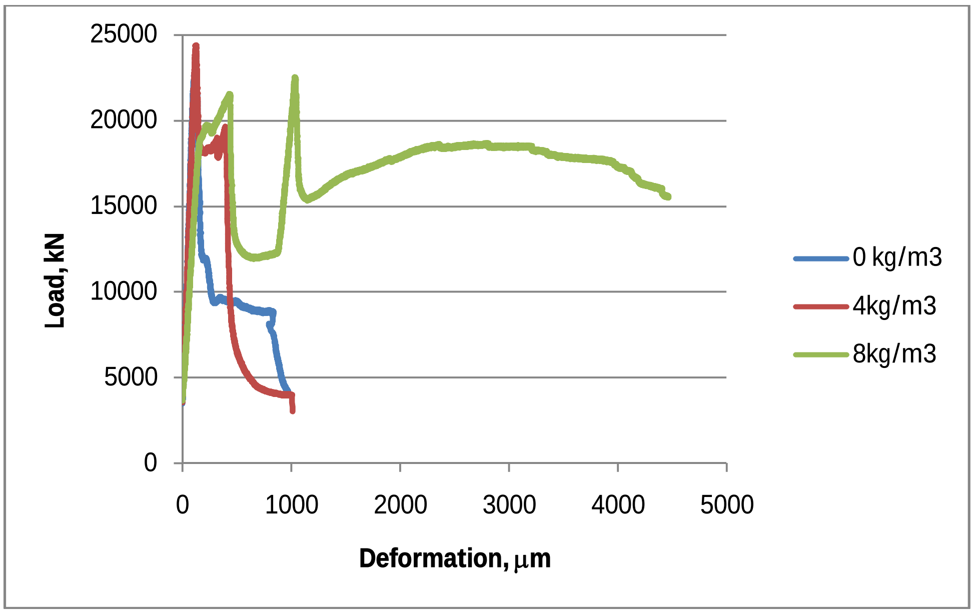

Fig.5 The function of load and vertical strain in fibreless, Mix 2 and Mix 3 specimens

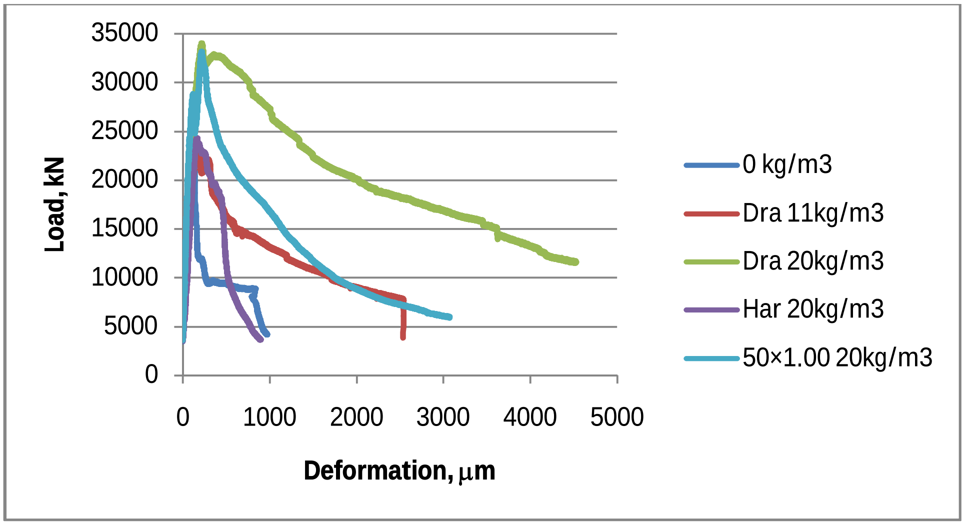

Fig.6 The function of load and vertical strain in fibreless, Mix 4, Mix 5, Mix 6 and Mix 7 specimens

The critical fracture energy G_{Fc} can be obtained from equation (2), if instead of work A required for specimen failure work A' required to open the critical crack width ($CMOD_C$) is used. Then characteristic length l_{ch} can be obtained from equation (3):

$$l_{ch} = \frac{EG_{Fc}}{f_t^2} \text{ [m]} \qquad (3)$$

However, if crack propagation direction is complex and unknown in specimens of other dimensions, crack trajectory is complicated, or multiple cracking occurs, the surface area after failure will be unknown. In that case fracture energy G_{Fc} and characteristic length l_{ch} cannot be obtained in the standard procedure (dividing work-of-fracture by cracked surface area). The answer to this problem was sought in the test described in this article and characteristic lengths were calculated not according to fracture energy, but according to work-of-fracture A at the first peak stress.

Table 6 Characteristic volume, area A_{ch} and l_{ch} of concrete specimens

Marking	Characteristic volume V_{ch}, m^3	Average characteristic length l'_{ch}, mm	Characteristic area A_{ch}, m^2	Average characteristic length l''_{ch}, mm
Mix 1	0,004297	163	0,03069	175
Mix 2	0,004399	164	0,03142	177
Mix 3	0,007501	196	0,05358	231
Mix 4	0,006386	186	0,04561	214
Mix 5	0,008247	202	0,05891	243
Mix 6	0,005680	176	0,04057	201
Mix 7	0,005016	171	0,03583	189

However, if work-of-fracture A is used instead of fracture energy G_{Fc} in equation (3), then characteristic volume v_{ch} (m^3) is obtained instead of characteristic length (Table 6).

$$v_{ch} = E \cdot A / f_t^2 \ [\mathrm{m}^3] \qquad (4)$$

In this case the average characteristic length l''_{ch} can be calculated by deriving a cube root of characteristic volume v_{ch}. From literature (Hadjab-Souag et al. 2007) it is known, that characteristic length of concrete is proportional to the length of fracture zone l_{FPZ}, which is larger than the width of fracture zone W_{FPZ} at the ratio 9:3.5. The side that limits the characteristic volume (also the entire volume of fracture zone above the tip of the crack) is of the same length as the length of the crack. So, in order to calculate the characteristic area A_{ch} (Table 6) it would be logical to divide v_{ch} by the length of crack l''_{ch} (in our case 140 mm). After extracting a square root of A_{ch} the side of average characteristic area l''_{ch} is obtained. From literature (Hadjab-Souag et al. 2007) it is known that the length of fracture zone l_{FPZ} and proportional characteristic length l_{ch} is 2.57 times bigger than the width of fracture zone W_{FPZ}. Thus, the average length l''_{ch} should be multiplied by $\sqrt{2.57}$, and hence the real characteristic length l_{ch} is obtained. When the characteristic length is calculated according to the work-of-fracture A (equation 3), then the critical fracture energy G_{Fc} can be calculated:

$$G_{Fc} = \frac{l_{ch} f_t^2}{E} \qquad (5)$$

If the actual fracture energy is unknown, the exact change of fracture energy can be obtained from the ratios of changed work A because work-of-fracture and energy are absolutely proportional.

Knowing that the average side having the characteristic length l''_{ch} is equal to one-third of the average length of fracture zone FPZ" (Table 7) the actual length of fracture zone l_{FPZ} and respectively the width W_{FPZ} (because l_{FPZ}:W_{FPZ}= 9:3.5) can be obtained by multiplying the length l''_{ch} by $\sqrt{2.57}$ (Table 7). In our case we found that at crack initiation time the length of fracture zone l_{FPZ} of fibreless concrete was 84 mm above the tip of that crack. In specimens Mix5 this length was the biggest and reached 111 mm.

The effect of fibres on reduced brittleness of concrete can be estimated according to the obtained characteristic length l_{ch} (Table 6) before crack initiation. According to literature (Hadjab-Souag et al., 2007), the characteristic length l''_{ch} is inversely proportional to concrete brittleness. The characteristic length l''_{ch} in specimens Mix 2 was similar to the length in fibreless specimens Mix 1, but in specimens Mix 3 this length increased 24%. Therefore, we may state that sufficient amount of polypropylene fibres can reduce the brittleness of concrete because the fibres can absorb the tensile stress and prevent concrete defects from joining the major concrete crack.

Table 7 Length and width of FPZ in concrete specimens (when l_{FPZ} : W_{FPZ} = 9 : 3,5)

Marking	Average length of fracture zone $l`_{FPZ}$ at V_{ch}, mm	Average length of fracture zone l''_{FPZ} at A_{ch}, mm	Length of fracture zone l_{FPZ} at A_{ch}, mm	Width of fracture zone W_{FPZ} at A_{ch}, mm
Mix 1	48,9	52,5	84,2	32,7
Mix 2	49,2	53,1	85,1	33,1
Mix 3	58,8	69,3	111,1	43,2
Mix 4	55,8	64,2	102,9	40,0
Mix 5	60,6	72,9	116,9	45,4
Mix 6	52,8	60,3	96,7	37,6
Mix 7	51,3	56,7	90,9	35,4

After the formation of the crack, plastic failure of specimens reinforced with polypropylene fibres can be seen by a naked eye (Figure 7). The increase of length l_{ch} from 7 to 28% in specimens reinforced with steel fibres can be explained in a similar way. In specimens Mix 5, Mix 6 and Mix 7 reinforced with 20 kg/m^3 of different type steel fibres the length l_{ch} as well as the plasticity of concrete increased 28%, 13% and 7% respectively.

Dra 2 (Mix 5)

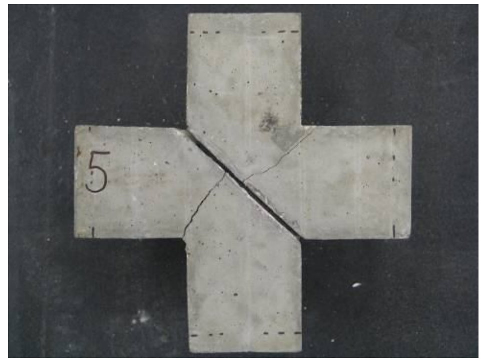

Har (Mix 7)

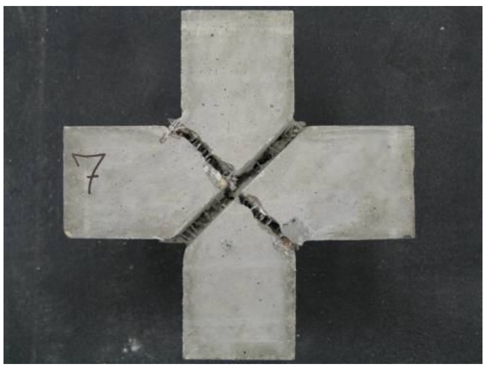

Poliprop 2 (Mix 3)

Fig. 7 Different failure of specimens due to the effect of different fibres or different amount of fibres

Conclusions

1. The article presents the method of calculating the characteristic length of concrete (and fibre reinforced concrete) specimens subjected to combined stress according to the characteristic volume of fracture zone. This method can be used if the work-of-fracture A is estimated experimentally.

2. Test results revealed that fibres can affect not only concrete fracture but also tensile strength because the use of fibres increased characteristic length l_{ch} of the specimens and the load value at the first peak.

3. Fibres with round cross-section used to reinforce concrete specimens subjected to combined stress change the character of the fracture because they detain initial crack propagation and cause other cracks to appear until specimen failure occurs.

4. All the fibres increased the elastic and plastic fracture energy of the specimens. Fibres in specimens Mix 5 (20kg/m^3) increased the elastic energy before the first peak stress by ~ 3 times, and the total energy necessary for specimen failure by 11 times.

5. For specimens subjected to combined stress the vertical strain and the critical width of the crack $CMOD_C$ at the first peak stress was bigger than in fibreless specimens 48% and 73% respectively.

References

1. Appa Rao, G., Raghu Prasad, B. Influence of type of aggregate and surface roughness on the interface fracture properties. Materials and Structures. Vol. 37, June 2004, p. 328-334.
2. Bakar, M., Skrzypek, K. Effect of Kaolin and Polyurethane on the Fracture and Thermal Properties of Epoxy Based Compositions. Materials Science. Vol. 13, No. 1. 2007, p. 39-42.
3. Bažant, P., Fellow, ASCE. Analysis of Work – of – Fracture Method for Measuring Fracture Energy of Concrete. Journal of Engineering Mechanics / February 1996, p. 138-144.
4. Gettu, R., Garcia-Alvarez, V. O., Aguado, A. Effect of aging on the fracture characteristics and brittleness of a high-strength concrete. Cement and Concrete Research. Vol. 28. No. 3, 1998, p. 349-355.
5. Guinea, G. V., El-Sayed, K., Rocco, C. G., Elices, M.., Planas, J. The effect of the bond between the matrix and the aggregates on the cracking mechanism and fracture parameters of concrete. Cement and Concrete Research 32, 2002, p. 1961-1970.
6. Hadjab-Souag, H., Thimus, J.-Fr., Chabaat, M. Detecting the fracture process zone in concrete using scanning electron microscopy and numerical modelling using the nonlocal isotropic damage model. Canadian Journal of Civil Engineering. NRC Research Press, 34, 2007, p. 496-504.
7. Hu, X., Duan, K. Influence of fracture process zone height on fracture energy of concrete. Cement and Concrete Research 34, (2004), p. 1321-1330.
8. Ioannides A., Concrete pavement analysis: the first eighty years, International Journal of Pavement Engineering, Vol. 7, No. 4, December 2006, p. 233-249.
9. Karihaloo, B. L. Fracture Mechanics and Structural Concrete. Concrete Design and Construction Series. Longman Scientific & Technical, Harlow,1995, 330 p.
10. Khalfallah, S. Tension stiffening bond modelling of cracked flexural reinforced concrete beams. Journal of Civil Engineering and Management. 14(2), 2008, p. 131-137.
11. Šalna, R.; Marciukaitis, G. 2007. The influence of shear span ratio on load capacity of fiber reinforced concrete elements with various steel fiber volumes. Journal of Civil Engineering and Management 13(3): 209–215.
12. Wang, Y. Toughness characteristics of synthetics fibre-reinforced cementitious composites. Fatigue & Fracture of Engineering Materials & Structures. 21, 1998, p. 521-532.
13. Zhang, J., Li, V. C. Simulation of crack propagation in fibre-reinforced concrete by fracture mechanics. Cement and Concrete Research 34, 2004, p. 333-339.

14. Zhang, D, Wu, K. Fracture process zone of notched three-point-bending concrete beams. Cement and Concrete Research 29, 1999, pp 1887-1892.
15. Žiliukas, A., Augonis, A. Assessment of concrete fracture in case of two-axis loading. Vilnius Gediminas Technical University, Lithuanian Academy of Science, International Association for Bridges and Structural Engineering, European Council of Civil Engineers ... [et al.]. Vol. 2. Vilnius : Technika, 2007. p. 851-856.
16. Yon, J, Hawkins, N, Kobayashi, A. Comparisons of concrete fracture models. Journal of Engineering Mechanics. March 1997, pp 196-203.